ACCURATE BEAM MODELING USING SPARSE REPRESENTATIONS OF VLA HOLOGRAPHY MEASUREMENTS

J. N. Girard[1], K. Iheanetu[2], O. M. Smirnov[2,3], K. M. B. Asad[3,2,4], M. de Villiers[3], K. Thorat[2,3], S. Makhathini[3,2] and R. Perley[2,5]

Abstract. Accurate knowledge of radio antenna beam pattern is critical for deep, wide-field imaging and modern data calibration. Being one of the primary "direction-dependent" effects which also depends on time and frequency, it limits the maximum reachable dynamic range in an image. Accurate models of the beam beyond the first null are therefore required to limit the amount of artifacts around offset sources. We present in this work, two methods relying on sparse representation of the VLA antenna holography beams. Compared to current reference model for this antenna, we show that our model provide accurate beam model that can be used for modern radio data calibration.

Keywords: interferometry, radioastronomy, holography, sparsity, beam, calibration

1 Introduction

The current and future large radio facilities such as the Low-Frequency Array (LOFAR – van Haarlem et al. (2013)) and the Square Kilometre Array (SKA – Dewdney et al. (2009)), in addition to bringing accurate measurements, also pose a challenge in advanced calibration. To the rescue, Radio Interferometer Measurement Equation mathematical framework (Hamaker et al. (1996); Smirnov (2011)) provides a simple way to represent the various and complex "direction-dependent" and "direction-independent" effects that distort the radio signal between the source and the induced voltages in radio antennas. One of these effects is caused by the radio antenna primary beam which highly depends on direction, frequency and time. Classical calibration is sufficient when imaging is performed inside the antenna main lobe, but deep, wide-field imaging outside the beam first null is limited by calibration artifacts. The latter will appear in radio images as structures surrounding offset sources. Further time and frequency integration can not mitigate these artifacts as they are due gain variation from an offset source crossing the irregular regions of the primary beam (side lobes, nulls, etc.).

Therefore, modern interferometric calibration nowadays includes correction for the spatial, temporal and spectral behaviour of the primary beam pattern. Its model should be simple and representative of the real antennas that are used for the observation. We will present in this study, the antenna beam models we derived for the Very Large Array (VLA) antennas.

2 Beam holography

First, radio antenna beam patterns can be obtained using numerical electro-magnetic simulations using ray optics or Maxwell equations to provide a theoretical model of the beam derived from the geometry of the antenna itself. For the VLA, the *CASSBEAM* model (Brisken (2003)) relies on the description of mechanical parameters of the antenna reflector, prime focus and struts. Such model gives a theoretical description of the beam assuming that all antennas of the array are identical. Another method consists of using "Holography"

---

[1] AIM, CEA, CNRS, Universit Paris-Saclay, Universit Paris Diderot, Sorbonne Paris Cit, F-91191 Gif-sur-Yvette, France

[2] Department of Physics and Electronics, Rhodes University, PO Box 94, Grahamstown, 6140, South Africa

[3] South African Radio Astronomy Observatory, 3rd Floor, The Park, Park Road, Pinelands, Cape Town, 7405, South Africa

[4] Department of Physics and Astronomy, University of the Western Cape, Bellville, Cape Town, 7535, South Africa

[5] NRAO, Charlottesville, USA

measurements to derive the effective radiation pattern of each antenna under test. In the interferometric array, some of the antennas are used as "reference" antennas whereas the remaining are used as "target" antennas. Using a known point radio source, the "target" antennas perform a raster scan around the radio source while "reference" antennas are kept on the source. The signal measured from the baselines involving the two types of antennas will be modulated by the beam pattern of the "target" antenna. Holography beams are then produced by following the data reduction methods described in Perley (2016).

Figure 1 depicts the comparison between the observed holographic beam pattern of the VLA antenna 5 at one typical frequency of 1008 MHz and the idealized beam pattern from the *CASSBEAM* model. The overall morphology of the beam can be correctly reproduced except for the Mueller matrix parameters $I \rightarrow Q$, $I \rightarrow U$ which display a higher level of noise and some residual rotation. *CASSBEAM* correctly represents the main features that are characteristic of the VLA antenna: four-fold petal distribution of the first side lobes, the beam squint (Chu & Turrin (1973); Uson, Juan M. & Cotton, W. D. (2008); Perley (2016)). However, by inspecting all frequency channels of the L-band from 1008 to 1908 MHz, a strong oscillating frequency "ripple" (with a period of 17MHz over the L-band) is present in addition to the geometrical λ/D scaling of the beam size. This effect is most likely due to standing waves occurring between the antenna primary reflector and the subreflector. Such effect is not modelled by the *CASSBEAM* model.
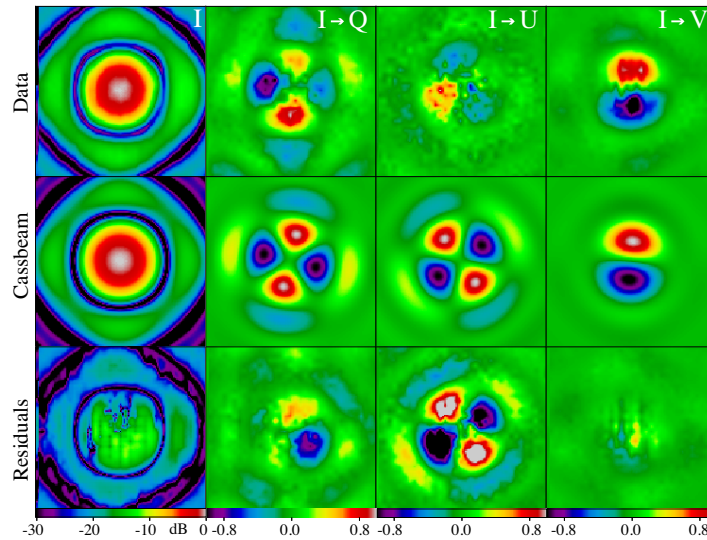

Fig. 1. Morphology of the Holography beam pattern compared to the *CASSBEAM* model at 1008 MHz. In each row are represented the Mueller matrix element (I, $I \rightarrow Q$, $I \rightarrow U$, $I \rightarrow V$) deduced from the holographic measurements *RR RL LR LL*. (top row) Holography data for Antenna 5 and (middle row)*Cassbeam* model (middle row); the last row depicts the residual level (in dB unit for I). Normalization of the beam patterns enables better visualization.

To address this effect, improved geometrical modeling was performed in Jagannathan et al. (2018) by fitting the *CASSBEAM* model to the holography data. Fitted parameters can be used to interpret the observed effects (such as the frequency ripple) in terms of variations of the antenna geometry. Mapping frequency-dependent distortions of the beam onto geometrical interpretation may be questionable. As a consequence, a more representative "independant" and accurate modeling of the antenna pattern is necessary to insure correct representation of the beam at all frequencies.

3 Methodology

Sparse representations can be applied for data representation and data reconstruction. The sparse representation of a signal is obtained by searching for the convenient space in which the data can be represented by as few coefficients as possible. While the Fourier space allows for sparse representation of oscillating signals, we have to find the correct space (and the associated transform) which can provide the necessary and sufficient number of coefficients that represent the beam pattern, and its variations in direction and frequency.

For this study, we used three approaches: i) a "data-driven" decomposition using Principal Component Analysis (PCA) implemented with Singular Value Decomposition (SVD) as depicted in Young et al. (2013) and

Mutonkole & de Villiers (2015) with the "Characteristic Beam Function Patterns" (CBFP)ii) an "orthonormal basis" decomposition of the antenna beam pattern on precomputed 2D Zernike polynomials and iii) a denoising of the holography cube. In the first approach, we derive a series of "eigenbeams" and their corresponding coefficients. PCA/SVD allows to determine the most adequate set of axes (i.e. basis vectors) to represent a dataset. The basis is virtually dependent on each dataset as it returns the best eigenbeams (and the corresponding coefficients) in the decreasing order of "energy", making low-rank approximations really straightforward to obtain. In the second approach, we performed a projection of the holography beam onto the Zernike polynomials which are adequate to represent information with circular symmetry. These two methods are different in nature and brought different results. The third exploits the fact that the antenna primary beam is linked to the antenna aperture illumination through a Fourier transform. We took the inverse Fourier transform of the holography beam at each frequency to obtained the effective illuminated disk with some non zero values leaking outside the aperture illumination. We thresholded the values outside this aperture before performing a Fourier transform back to the primary beam. As a results, we obtained partially denoised version of the holography beam.

For the first two methods, we "compressed" the spatial information by performing low-rank approximations on the respective coefficients by keeping only the "relevant" coefficients which contains most of the information of the beam. We get a series of coefficients per frequency, which can again be compressed along the frequency axis. The presence of a dominating ripple in VLA antennas suggests to use the Discrete Cosine Transform (DCT) to represent the frequency behaviour of the series of coefficients (per spatial mode) with as few DCT coefficients as possible. Beam patterns are highly compressible spatially and spectrally using this combination of a spatial decomposition of the beam and the spectral decomposition of the corresponding coefficients.

4   Results

For each methods (PCA/SVD, Zernike and thresholding), we computed the full decomposition of the beams into coefficients and we compared the associated low-rank approximations to the optimized *CASSBEAM* model from Jagannathan et al. (2018). Figure 2 represents the reconstruction residuals (in dB) between the original holography beam and each methods used at 1008, 1408 and 1908 MHz. For both PCA/SVD and Zernike, we reconstructed the approximated holography cubes using the first 20th spatial coefficients (SVD or Zernike) and 50 DCT coefficients. First row shows the difference between holography and the optimized *CASSBEAM* model, followed by the PCA/SVD reconstruction, Zernike reconstruction and the thresholded recontruction (HT), with the same colorscale. Among the four methods, PCA/SVD provides the lowest reconstruction residuals over the full band. The Zernike decomposition seems to show good results at the low frequencies only. For all methods, larger errors are mostly located around beam nulls, due to the fact that they are difficult to reproduce accurately with low-rank approximations. The optimized *CASSBEAM* displays moderate reconstruction residuals but shows better results than the denoised holography cube.

By construction, PCA/SVD is the most accurate model for the set of holography beams we have. To test the robustness of these basis, we tried to produce a "common" set of eigenbeams that could represent the behaviour of multiple "target" antennas. We noticed that performances are degraded as a larger number of coefficients are required to compensate for the inadequacy of the "common" basis with respect to each antenna behaviour. With this basis, results are equivalent to that obtained with the Zernike basis.

5   Conclusions

Modern interferometer calibration requires an accurate knowledge of the radio antenna beam pattern to enable widefield and deep imaging. It is critical to calibrate the data with accurate (but compressible) representation of the beam. Using sparse representations and simple decomposition methods, we were able to find accurate representations of holography beam cubes for all VLA antennas under study with two methods of representation and compression. The SVD/PCA is showing the best results compared to the other representations. The derivation and the statistical study over all antennas as well as the evaluation of compressibility factors for each methods will be available in a featured article currently under review.
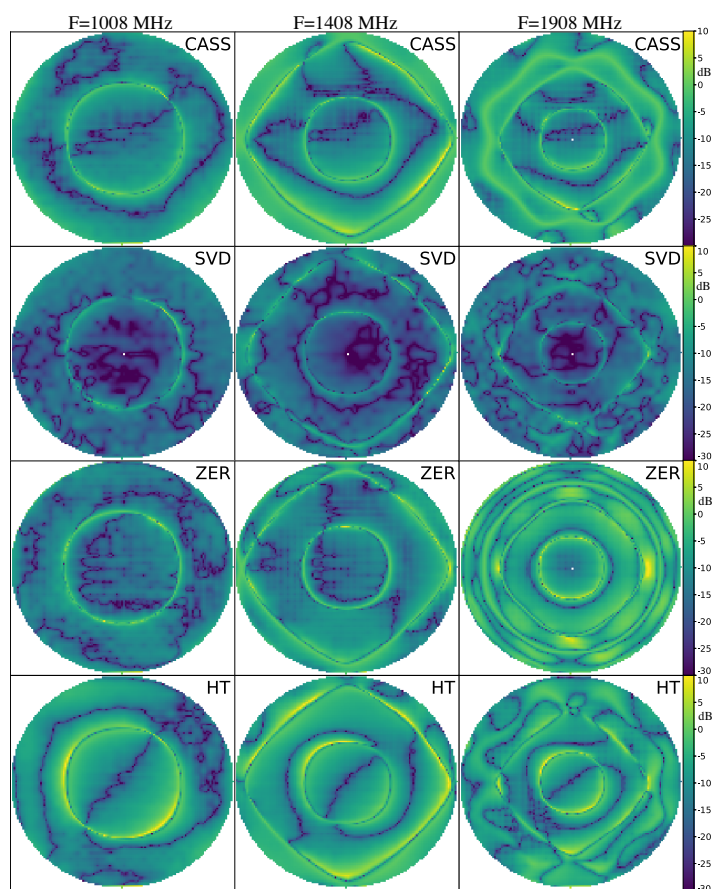
Fig. 2. Relative residual reconstruction errors for antenna 6 represented in the range [-30 dB, 10 dB] at f=1008, 1408, 1908 MHz. Residuals are computed from the difference of the original holography beam and the optimized *CASSBEAM* model, Principal Component Analysis with SVD (SVD), Zernike (ZER) and Threshold (HT) reconstructed beams. Reconstruction quality with *RR* and *LL* beams are equivalent.

References

Brisken, W. 2003, EVLA Memo

Chu, T.-S. & Turrin, R. 1973, IEEE Transactions on Antennas and Propagation, 21, 339

Dewdney, P., Hall, P., Schilizzi, R., & Lazio, T. 2009, Proceedings of the IEEE, 97, 1482

Hamaker, J. P., Bregman, J. D., & Sault, R. J. 1996, A&AS, 117, 137

Jagannathan, P., Bhatnagar, S., Brisken, W., & Taylor, A. R. 2018, AJ, 155, 3

Mutonkole, N. & de Villiers, D. I. L. 2015, in 2015 9th European Conference on Antennas and Propagation (EuCAP), 1–5

Perley, R. 2016, EVLA Memo 195

Smirnov, O. M. 2011, A&A, 527, A106

Uson, Juan M. & Cotton, W. D. 2008, A&A, 486, 647

van Haarlem, M. P., Wise, M. W., Gunst, A. W., & et al. 2013, A&A, 556, A2

Young, A., Maaskant, R., Ivashina, M. V., de Villiers, D. I. L., & Davidson, D. B. 2013, IEEE Transactions on Antennas and Propagation, 61, 2466